

INVESTIGATIONS OF FLAKEBOARD MAT CONSOLIDATION. PART I. CHARACTERIZING THE CELLULAR STRUCTURE

Christopher A. Lentz

Graduate Research Assistant

and

Frederick A. Kamke

Associate Professor

Virginia Polytechnic Institute and State University
Department of Wood Science and Forest Products
Brooks Forest Products Center
1650 Ramble Road
Blacksburg, VA 24061-0503

(Received July 1995)

ABSTRACT

As the wood-based composites industry continues to grow larger and more advanced, there is a need for a more fundamental understanding of material behavior during the hot-pressing process. This work describes the development and implementation of a method for quantifying the cellular structure of a flakeboard mat. Cross-sectional images of narrow mat sections and 6-in. × 6-in. mats were obtained, and structural parameters were quantified using computer image analysis techniques. Mat structure was analyzed with respect to: the percent area of mat cross section occupied by voids, the size and shape of individual voids, and the distribution of void size and shape. For mats formed with flakes oriented both randomly and parallel to the image plane, there was no significant difference in the average area of individual voids between the narrow mat sections and 6-in. × 6-in. mats. However, a significant difference in average area of individual voids between the two mat types was observed in mats formed with flakes oriented perpendicular to the image plane. Void size was not significantly affected by the direction of flake orientation. Void shape was significantly affected by both the method of mat formation and the direction of flake orientation.

Keywords: Oriented strandboard, wood flake mats, consolidation, hot-pressing, image analysis.

INTRODUCTION

The network of flakes and void spaces that comprises the structure of a wood flake mat is controlled by several variables, among which flake dimensions and forming procedures are of primary importance. The void structure created by the interaction of raw material and mat formation parameters has many important implications for evolution of the ultimate properties of the final product. The size and distribution of voids in the mat as it is compressed will affect the transfer of heat and moisture within the panel during manufactur-

ing. The horizontal and vertical density distributions within a panel will also be significantly affected by the distribution of void area, as will the mechanical properties.

The structure of a wood flake mat resembles that of a cellular material. In such an analogy, the cell walls of the material are composed of the flakes, and the voids are the spaces between the flakes. The mechanical properties of such cellular materials are governed by the cellular geometry, or arrangement of cells, and the properties of the solid cell-wall substance. The influence of environmental variables is restricted to the cell-wall substance; and the ef-

fects of time, temperature, and moisture are combined in the viscoelastic response of the cell-wall material (Wolcott et al. 1990). The cellular geometric structure gives rise to the nonlinear response that is characteristic of cellular materials when loaded in compression. Separating the nonlinear response of the cellular structure from the viscoelastic behavior of the cell-wall material has been demonstrated to be an effective route in simplifying the understanding of the complex mechanical behavior of cellular materials (Gibson and Ashby 1988; Meinecke and Clark 1973; Warren and Kraynik 1987; Wolcott 1989). Theories based on this principle have been shown to effectively model the compressive stress-strain behavior of many natural and synthetic cellular materials based on cell geometry and mechanical properties of the cell-wall substance (Ashby 1983; Gibson and Ashby 1988; Gibson 1989b; Meinecke and Clark 1973; Warren and Kraynik 1987; Wolcott 1989). Thus it was the goal of this research to characterize the cellular structure of wood flake mats in the interest of modeling the consolidation of wood flake mats using theories of cellular materials. A method for observing the gross macroscopic structure of a flakeboard mat prior to and during consolidation was developed using computer image analysis techniques to quantify the parameters necessary to define a cellular structure for flakeboard mats. The results of this research will be used specifically as supporting information in modeling the stress-strain behavior of wood flake mats during consolidation. The results of the modeling investigations will be discussed in a subsequent publication on modeling mat consolidation using theories of cellular materials. However, the information provided herein also has valuable implications for other areas of wood-based composites research, including heat and mass transfer and vertical and horizontal density distributions.

Characterizing cellular solids

Cellular materials are common in both natural and man-made settings. While synthetic cellular materials exist primarily for their

cushioning, insulating, padding, and packaging functions, natural cellular materials fulfill all of these functions and more. Nature also uses cellular materials such as coral, bone, and wood to create large, load-bearing structures, something which modern man creates with dense solids like metal, glass, and concrete (Ashby 1983). Cellular materials have considerable engineering potential, but understanding their mechanical properties is not as straightforward as in dense solids.

Cellular solids can be isotropic or anisotropic, and this tropicity is a direct result of the arrangement of cells and the relationship between the cell dimensions in different directions (Gibson and Ashby 1988). Much of the information necessary for determining the properties of conventional solids can be found in a description of the material of which the cellular material is made, and the rest can be obtained from optical or scanning micrographs (Gibson and Ashby 1988).

Characterizing wood composite mats

Very little work has been done to characterize the network of flakes and void spaces that comprise the cellular structure of a wood flake mat. A related topic, the density distribution within a wood composite mat, however, has been the topic of significant inquiry. Kelly (1977) reported on several studies into the effects of various pressing parameters on the vertical density distribution of nonveneered structural panels. Harless et al. (1987) developed a model to predict the vertical density profile of particleboard, simulating the physical and mechanical processes occurring in the mat during pressing. Suchsland (1959, 1962) was perhaps the first to investigate the horizontal density distribution in wood composites, determining that flake geometry will affect the relative void volume in a mat. Suchsland and Xu (1989, 1991) continued their investigations to develop a model for simulation of the horizontal density distribution in flakeboard. From this research, it was concluded that both the internal bond (IB) and thickness swell (TS) properties were directly affected by

the horizontal density distribution (1989, 1991).

Interest in predicting the compression behavior of wood flake mats has led to the development of a probability-based model to describe a randomly packed, short-fiber-type wood composite (Dai and Steiner 1994a, 1994b; Steiner and Dai 1994). The model uses the approach that the structural properties of a randomly formed flake network are random variables, essentially characterized by Poisson and exponential distributions, and predicts the distribution of: number of flake centers per unit of layer area, flake area coverage, free flake length, and void size (area as viewed from above). Dai and Steiner (Dai and Steiner 1994a, 1994b; Steiner and Dai 1994) determined that the expected structural properties of a random flake layer can be adequately modeled from average flake length and width, total flake number, and total layer area. Lang and Wolcott (1996) developed a Monte Carlo simulation procedure that predicts the number of strands in the centroids of imaginary strand columns, the vertical distance between adjacent strands, and the position of the column centroid in relation to strand length based on data from laboratory mats. This simulation procedure was effectively incorporated into a model that predicts the static stress-strain behavior of randomly oriented strand mats.

EXPERIMENTAL METHODS

Wood flake mats

Two types of wood flake mats were used in this study: 210-mm by 13-mm (9-in. by 0.5-in.) narrow mat sections, referred to as model mats, and 152-mm by 152-mm (6-in. by 6-in.) square laboratory-size mats. Two types of wood flake furnish were used to form the mats: yellow-poplar (*Liriodendron tulipifera*) flakes cut on a laboratory disk flaker, and commercially prepared OSB flakes. Commercial flakes were comprised of 60% softwood, 30% low density hardwood, and 10% high density hardwood. All flakes were screened using an oscillating screening bed to remove flakes with an average

width of 3.2 mm (0.13 in.) or less. Three wood flake mat configurations were examined in this study: yellow-poplar flake model mats (YP-MODEL), yellow-poplar flake 6-in. × 6-in. mats (YP6X6), and commercial flake 6-in. × 6-in. mats (COM6X6), as shown in Fig. 1. Five random and ten oriented model mats were created. Of the ten oriented model mats, five were designed with the longitudinal axis of the flakes running parallel to the image plane (x-direction) and five had the longitudinal axis of the flakes running perpendicular to the image plane (y-direction). In this way, model mats were created to simulate cross sections of a single layer oriented flake mat both in and across the direction of flake orientation.

The use of image analysis techniques to quantify mat structural parameters required that the edges of the mats be vertical and planar. The narrow mat sections were designed specifically for this purpose and allowed for extra measures to be taken that increased the contrast between flakes and voids. The model mats were designed to simulate a narrow vertical section of a flakeboard mat. In these model mats, the voids were prismatic and continuous from the front to the back edge of the mat. Thus when observing an image of a model mat edge, the fraction of the image occupied by spaces between flakes was roughly the same as the void volume fraction in the model mat. To increase the contrast between the flakes and voids, wood blocks were painted with flat white latex paint prior to flaking so that the flakes would have one white edge. Figure 2 illustrates the methodology used in the design of the model mats. To simulate a straight-grained flake with x-y-z dimensions of 75 mm (2.95 in.) by 25 mm (0.98 in.) by 0.7 mm (0.0275 in.) intersecting a narrow mat section at different angles from the x-direction, model mats were created using rectangular flakes with various angles of grain orientation. Flakes were machined with grain orientations of 0, 15, 30, 45, 60, 75, and 90 degrees from the longitudinal axis. By flipping the flakes over, a full 180 degrees of flake orientation could be realized. All flakes were 13 mm (0.5 in.) in the

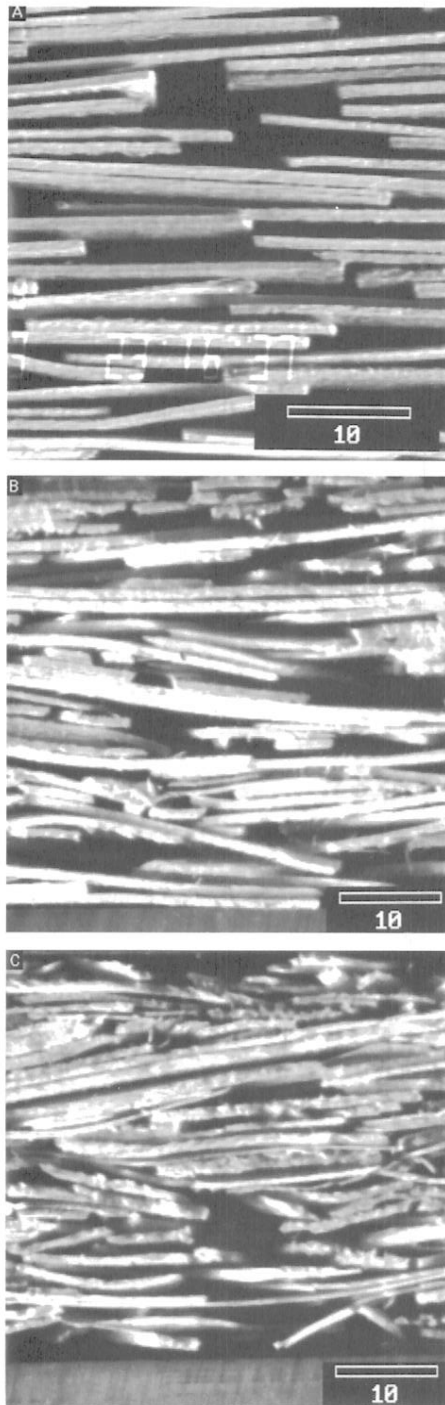


FIG. 1. Sample images of mat cross sections: a) YP-MODEL mat formed with flakes oriented randomly, b) YP6X6 mat formed with flakes oriented randomly, and c) COM6X6 mat formed with flakes oriented randomly. Calibration bars are in millimeters.

y-direction and approximately 0.7 mm (0.0275 in.) in the z (thickness) direction. Flake dimensions in the x-direction varied with grain orientation from 25 mm (0.98 in.) to 75 mm (2.95 in.). By varying the grain angle and length of the rectangular flakes as described, a model mat could effectively simulate a narrow “slice” of an actual mat with straight-grained flakes passing through the narrow section at any orientation from 0 to 180 degrees. The model mats were hand-formed in trays measuring 280 mm (11 in.) wide, 130 mm (5 in.) high, and 13 mm (0.5 in.) deep. A calibrated grid was superimposed on the inside of the tray to assist in the placement of the flakes. In forming the model mats, the grain orientation for each flake to be placed in the mat was chosen at random. For the randomly oriented model mats, flakes with grain angles from 0 to 180 degrees had an equal chance of being selected. For the model mats with flakes oriented in the x-direction, the random number determining the grain orientation was categorized such that approximately 70% of the flakes chosen had a grain orientation of 0°, 15% had a grain orientation of 15°, 10% had grain orientation 30°, and 5% had a grain orientation of 45°. Similarly, for the model mats with flakes oriented in the y-direction, 70% of the flakes had a grain orientation of 90°, 15% at 75°, 10% at 60°, and 5% at 45°. This convention was developed based on discussions with personnel in the OSB industry. A flake of the randomly determined orientation was then placed in the tray, aligning the left edge at a randomly determined position on the grid. In this manner, model mats were built up one flake at a time on a balance, to a target weight of 50 grams, providing a dry mat density of 590 kg/m³ (37.0 lb./ft³) at a thickness of 28.5 mm (1.13 in.). This thickness was chosen to maximize the number of voids visible in the images. The mats were transferred from the trays to an apparatus specially designed to maintain the integrity of the mat edges while the mats were compressed and images of the mat cross sections were recorded.

Nine 6-in. by 6-in. laboratory mats were

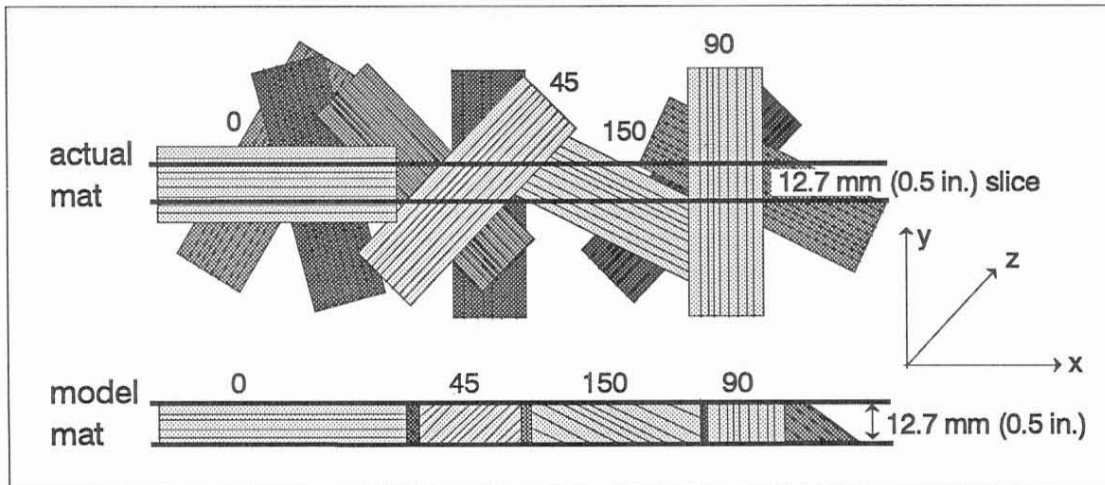


FIG. 2. Illustration of the methodology used in the design of model mats. Numbers represent angle of flake orientation in actual mat and angle of grain orientation in the model mat.

formed with commercial OSB furnish, of which four were randomly oriented and five were preferentially oriented. The orientation was performed using a 760-mm by 760-mm (30-in. by 30-in.) flake orienter by passing flakes between vibrating parallel metal plates into a deckle box. Four 6 × 6 mats were formed using laboratory manufactured yellow-poplar furnish. All 6 × 6 mats were hand-formed to an original size of 305 mm by 305 mm (12 in. by 12 in.) on a balance, to a target weight of approximately 400 grams, which provided a mat density of at least 590 kg/m³ (37.0 lb./ft³) at a thickness of 12.7 mm (0.5 in.). Because the dimensions of these mats would later be reduced, the target weight reflects additional furnish included to offset possible losses. The desired thickness for the 6 × 6 mats was thinner than that for the model mats because the procedure used to surface the mats was limited in the thickness it could accept. Due to this surfacing procedure, special measures were taken during mat formation. Inside the deckle box, the 6 × 6 mats were formed on top of two thin pieces of plywood: a 153-mm by 153-mm (6-in. by 6-in.) square that fit inside a 305-mm × 305-mm (12-in. by 12-in.) square containing a 153-mm by 153-mm square hole in the center. Two identical pieces of plywood were

placed on top of the finished mats. The mats were then compressed to a 50-mm (2-in.) thickness with a screw press and fastened in place with screws.

A commercial paper shear at the West Virginia University Department of Forestry was used to reduce the mat dimensions to 153 mm by 153 mm. This produced square mats, each with four surfaced, vertical edges suitable to obtain quality cross-sectional images. Each of the five oriented mats had two surfaced edges where the flakes were oriented across the face (x-direction), and two with the flakes oriented perpendicular to the face (y-direction).

Prior to image collection, each 6 × 6 mat was transferred to an apparatus constructed to keep all four mat edges square and intact while images of the mat edges were being obtained. This apparatus was essentially a four-sided plexiglass box attached at the corners and fixed at bottom to a 153-mm by 153-mm by 25-mm-thick aluminum plate. This device could be opened to insert and remove mats and was also used for later consolidation of the 6 × 6 mats. The 6 × 6 mats were reweighed prior to being placed in this device, and their mass was adjusted to achieve the target density. The moisture content of the mats was approximately 8.5%.

Image collection

Images of the mat edges were captured using a DAGE—MTI CCD 72 television camera equipped with a 50-mm 1:1.4 Cosmocar television lens. Magnification was achieved by inserting Cosmocar extension tubes between the camera and the lens. The television camera was networked with a WIN 486 microprocessor and image analysis system. Images were displayed on a Sony Trinitron® high resolution monitor. In the case of the model mats, the camera signal was routed through a time-date generator into a high resolution SVHS video recorder. The time-date generator stamped a stopwatch time onto the video signal for future correlation with load and deflection data. The image analysis software package used was Image 1/ AT® version 4.1 from Universal Imaging Corporation, with an image resolution of 480×512 pixels.

The apparatus containing the model mats was fixed to an MTS universal servohydraulic testing machine fitted with a 2270-kg (5000-lb.) load cell. The optical bench with attached camera was fixed to the table of the testing machine, and lighting was provided by two 250-watt photo floodlight bulbs with 10-inch convex metal reflectors. A 5-mm extension tube was used for magnification, providing a resolution of approximately $30\times$ on the video screen. This provided an image resolution of 52 to 56 pixels per mm^2 . The camera was maneuvered to record an area in the bottom center of the mat edge, and after the lighting and camera were fixed, the videocassette recorder was started. The measurement system was calibrated by measuring an object of precisely known dimensions on the mat edge. The actual dimensions of the object were then used to create a calibration file for that particular spatial configuration. The time-date generator and data acquisition system for recording load deflection information were then started simultaneously, followed by the testing machine. Each model mat was then compressed at a rate of 25 mm per minute until the maximum limit of the load cell was reached.

Because of the random nature of mat formation, uncompressed mats varied considerably in density. To facilitate comparisons between the images of mat cross sections, all mats were compressed to a density of approximately 250 kg/m^3 (15.6 lb./ft^3) prior to image collection. Images of the model mats were obtained by connecting the output of the video cassette recorder to the video input of the image analysis system and playing back the tape of the mat consolidations. The time at which each mat reached a density of 250 kg/m^3 was obtained from the accompanying load-deflection data file, and used as an indicator for when to "grab" an image from the videotape as it was played back into the imaging system. At the appropriate time, an image was acquired by averaging four consecutive frames.

Cross-sectional images of the 6×6 mats were obtained directly without the use of the video recorder, time-date generator, or the MTS machine. The mats were placed in the consolidation apparatus and the apparatus was configured to fix the mat density at 250 kg/m^3 . The consolidation apparatus was attached in a fixed position to the optical bench, and the lights and camera were fixed in a similar configuration as with the model mats, providing an image resolution of 40 pixels per mm^2 .

Image processing and measurement

Two image processing steps were carried out to prepare the images for measurement. An absolute foreground minus background ABS(F-B) logic procedure was carried out by loading a mat image and subsequently subtracting the corresponding white reference image. This procedure removed any areas or objects that were common to both images and also effectively inverted the contrast of the image. The gray scale values in the resulting image were the absolute values of the difference between the two images. A histogram stretch function was performed to bring more resolution to bear on the features of interest in the images.

The features of interest on the images were the voids in the mat structure. Specific mea-

TABLE 1. Number of mats tested, mat sides observed, voids measured, and the percent of observed mat area occupied by voids for each mat type at a mat density of 250 kg/m³.

Flake orientation Mat type	Random			Parallel to image plane		Perpendicular to image plane	
	YP model ¹	YP 6 × 6 ²	COM 6 × 6 ³	YP model	COM 6 × 6	YP model	COM 6 × 6
Number of Mats	5	4	4	5	5	5	5
Mat Sides Observed	5	16	16	5	10	5	10
Voids Measured	532	1,687	1,982	599	1,332	638	1,411
Percent of Observed Mat Area Occupied by Voids							
Mean	33.25	36.45	34.71	34.79	31.21	38.82	30.68
COV%	14.56	21.56	19.25	10.29	14.64	14.30	27.61

¹ YPMODEL is the designation for narrow mat sections formed from yellow-poplar furnish.

² YP 6 × 6 is the designation for 6 in. by 6 in. laboratory mats formed from yellow-poplar furnish.

³ COM 6 × 6 is the designation for 6 in. by 6 in. laboratory mats formed from commercial furnish.

surements of interest included: void count, void length, void diameter, void area, void shape, and total mat area occupied by voids. The procedure for measurement of the mat images was comprised of four steps: loading the processed mat image, loading the corresponding calibration file, thresholding the image, and initiating the object measurement function. A size filter was used to prevent objects smaller than 0.25 mm² from being included in the measurement. This was determined as the size below which objects could not be visually recognized as being voids. After the processed image and corresponding calibration file were loaded, the image was thresholded to determine a gray level that delineated the objects of interest from the rest of the image. The object measurement mode was then initiated, measuring all objects that satisfied the size filter within the outlined region of the image. For each object in each image, the following parameters of interest were logged to a data file for each of the objects measured: position (in x and y coordinates), area, percent area, hole area, percent hole area, perimeter, shape factor, chord length, chord angle, diameter, filter match, number of objects and region area.

RESULTS AND DISCUSSION

Percent mat area occupied by voids

The percent area of a mat cross section image that is occupied by voids is an indication

of the volume of voids in the associated three-dimensional mat. In the model mats, the rectangular flakes created voids that were prismatic and continuous through the y-direction of the mat, in which case the percent void area at the mat edge should be roughly the same as the percent void volume of the thin mat section. Table 1 lists the number of mats tested, number of mat sides observed, the number of voids measured, and the average percent of mat area occupied by voids for each mat type. The values of percent void area were quite similar for all mat types observed. Since all images were obtained with the mats at the same density, and thus roughly the same void fraction, the moderate differences between groups are likely the result of randomness in the formation techniques. With regard to percent mat area occupied by voids, a one-way ANOVA procedure determined that no significant differences existed among the seven mat types ($p > 0.10$).

Void size

The size of each void measured was characterized with respect to the area occupied, percent of total mat area occupied, chord length, diameter, and perimeter. The chord length measurement yields a measure of the greatest linear distance between any two points on the object (Universal Imaging 1991). The diameter of an object is defined by the software

TABLE 2. Individual void dimensions and shape as a function of flake orientation and mat type at a mat density of 250 kg/m³.

Flake orientation Mat type	Random			Parallel to image plane		Perpendicular to image plane	
	YP model	YP 6 × 6	COM 6 × 6	YP model	COM 6 × 6	YP model	COM 6 × 6
Area (in mm²)							
min	0.26	0.27	0.27	0.25	0.27	0.26	0.27
max	204.80	843.90	797.40	164.40	223.60	590.10	491.10
mean	7.93	8.34	6.76	8.84	5.66	10.08	5.25
cov%	245.60	399.28	386.39	223.64	257.95	377.68	379.05
DIAMETER (in mm)							
min	0.12	0.29	0.29	0.24	0.29	0.25	0.29
max	5.62	8.25	10.60	2.99	4.59	6.81	9.20
mean	0.51	0.69	0.71	0.45	0.68	0.54	0.73
cov%	107.84	84.06	80.28	84.44	72.06	101.85	72.60
CHORD LENGTH (in mm)							
min	1.04	0.69	0.71	1.04	0.71	0.94	0.69
max	77.26	87.76	87.21	74.68	86.22	76.58	84.25
mean	12.47	8.07	6.44	14.83	6.61	10.96	5.32
cov%	117.56	136.43	139.75	124.88	129.35	135.58	127.44
SHAPE FACTOR							
min	0.01	0.02	0.01	0.01	0.03	0.01	0.02
max	0.63	0.65	0.75	0.54	0.66	0.64	0.64
mean	0.12	0.24	0.27	0.10	0.25	0.15	0.29
cov%	66.67	54.17	48.15	70.00	52.00	66.67	41.38

as the thinnest portion of an object that roughly crosses the center of the object (Universal Imaging 1991).

Table 2 provides summary statistics for the dimensions and shape of the individual voids measured as a function of flake orientation and mat type. There was extreme variability in the area of the voids measured: ranging from 0.25 mm² to nearly 850 mm². The larger void sizes observed resulted from connections between adjacent voids. Any adjacent void areas that were not completely separated by flakes were grouped together and measured as one contiguous void. At a mat density of 250 kg/m³, the possibility of interconnections between voids is likely. The mats formed from commercial furnish contained voids that were on average smaller than the voids in the mats formed from YP flakes. The commercial furnish mats contained a much broader distribution of flake sizes than the YP flake mats. During mat for-

mation, the narrower and shorter flakes in the commercial furnish allowed for the creation of smaller voids than did the uniform YP flakes. This was manifested in a smaller observed average individual void area for mats formed of commercial furnish. A one-way ANOVA model comparing void area by mat type determined that significant differences existed between mat types ($P < 0.001$). Subsequent multiple comparisons by Tukey's honest significant difference (HSD) method ($\alpha = 0.05$) revealed that for the mats formed with flakes oriented perpendicular to the image, average area of voids for YPMODEL mats was significantly larger than the average area of voids for COM6X6 mats.

Histograms were also prepared to show the distribution of void area by mat type. Figure 3a illustrates the percent of total observed mat area occupied by voids as a function of void size for the three types of randomly oriented

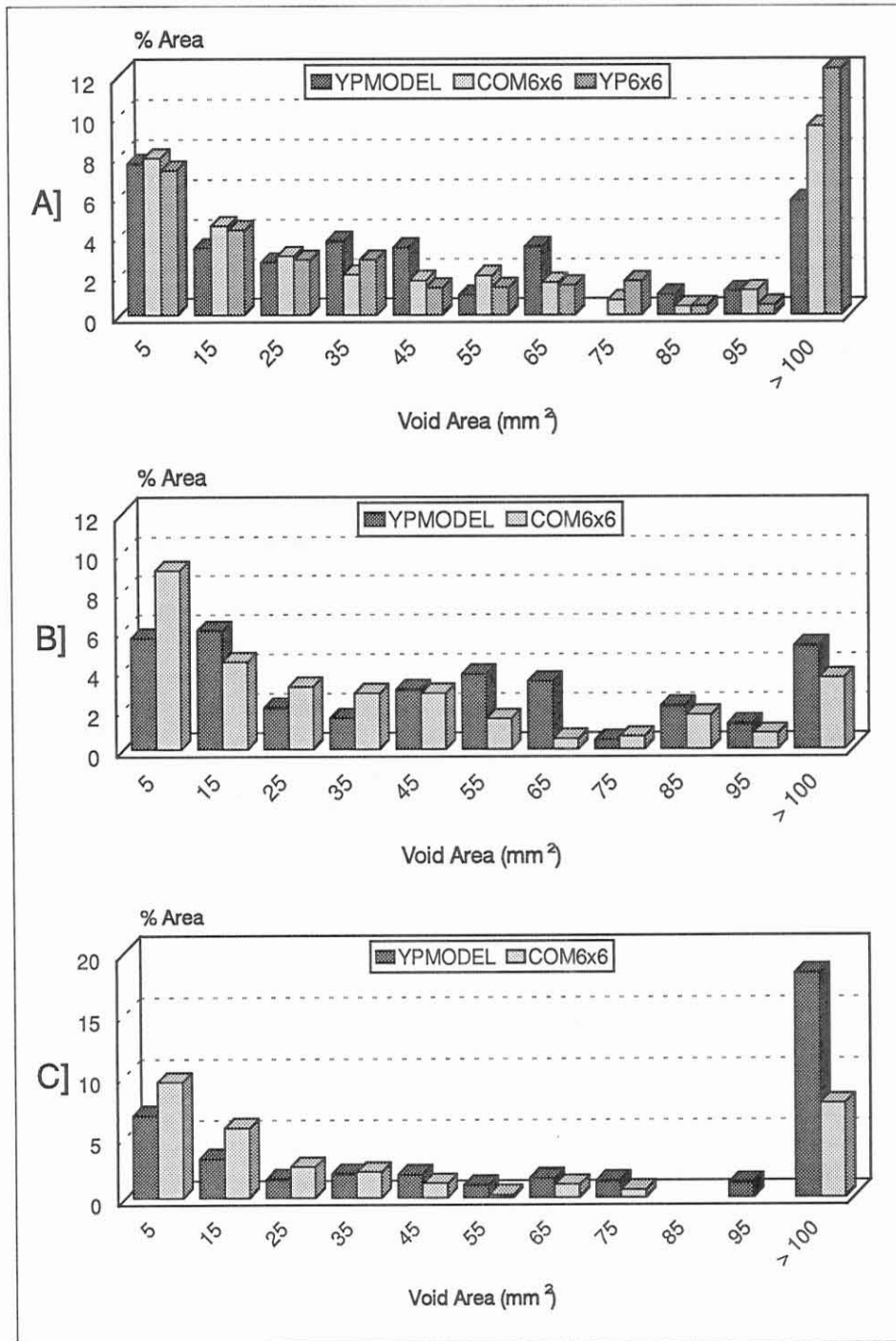


FIG. 3. Histograms depicting the distribution of void size for: a) mats formed with flakes oriented randomly, b) mats formed with flakes oriented parallel to the image plane, and c) mats formed with flakes oriented perpendicular to the image plane.

mats observed. The percent area is fairly evenly distributed among the size classes, with voids in the 0 to 10 mm² and > 100 mm² size classes occupying the largest amount of mat area. This visually reinforces the results of the statistical comparisons, where no significant differences in average void area were found to exist among mats with randomly oriented flakes. The only marked difference between the mat types existed in the > 100 mm² size class. This size class comprised 12% of the total mat area for the YP6X6 mats, compared to 9% for the COM6X6 mats, and 5% for the YPMODEL mats. Figure 3b shows the distribution of void area by size class for YPMODEL and COM6X6 mats with flakes oriented parallel to the image plane. This distribution is also fairly uniform across the size classes. COM6X6 and YPMODEL mats appear to have similar distribution shapes, underscoring the fact that no significant differences in average void area were revealed among mats with flakes oriented parallel to the image plane. Figure 3c shows the distribution of void area by size class for YPMODEL and COM6X6 mats with flakes oriented perpendicular to the image plane. A difference in the shapes of the distributions for the two mat types is evident. The proportion of mat area occupied by voids larger than 100 mm² is considerably higher for the YPMODEL mats than it is for the COM6X6 mats. This reflects the significant difference in average void size existing between these two mat types for this flake orientation. Consequently, the percent mat area occupied by voids less than 30 mm² is greater for the COM6X6 mats. Differences in the distributions of void sizes exhibited in the histograms reflect previously discussed differences in flake sizes between the different types of furnish used.

While void area was considered to be a reliable description of void size, each of the voids measured on the images was also characterized by its diameter and its chord length. Concerns raised by differences in diameter and chord length will be considered in the discussion of void shape to follow. In general, the YPMODEL mats had smaller diameters and longer

chord lengths than the COM6X6 mats (Table 2). This suggests that the YPMODEL mats had longer, thinner voids opposed to shorter, thicker ones for the COM6X6 mats. It is likely that this relationship also stemmed from the differences in flake size between the yellow-poplar flakes and the commercial furnish. A one-way ANOVA procedure comparing the average void diameter by mat type exposed significant differences among the mat types ($P < 0.0010$). Multiple comparisons of means by Tukey's HSD ($\alpha = 0.05$) method revealed significant differences in average void diameter between YPMODEL mats and COM6X6 mats at all three directions of flake orientation. Among the mats with random flake orientation, the average void diameter of the YPMODEL mats was significantly lower than that of both the YP6X6 and the COM6X6 mats. For both directions of flake orientation, the average void diameter of the YPMODEL mats was significantly less than that of the COM6X6 mats. No significant differences were found between flake orientations within the YPMODEL and COM6X6 mat types. Statistical comparisons were not provided for the chord length data because the relationship between mat types was almost exactly the inverse of that for diameter, i.e. the mats with the larger void diameters had shorter chord lengths.

Void shape

The shape factor allows objects to be classified by the extent of their roundness, wherein a shape factor of 1.0 represents a perfectly round object and a shape factor of 0.0 represents an infinitely thin object. An object's shape factor is defined as the area of the object divided by the area of a circle having a diameter equal to the perimeter of the object divided by pi (Eq. 1):

$$\text{shape factor} = \frac{4\pi a}{p^2} \quad (1)$$

where a = object area and p = object perimeter. Table 2 also gives summary statistics for the shape factor of voids for the seven combina-

tions of mat type and flake orientation studied. A one-way ANOVA model comparing the average shape factors for all mat types indicated that significant differences existed among the mat types. Multiple comparisons by Tukey's HSD method ($\alpha = 0.05$) revealed significant differences in the average shape factor between the YPMODEL and COM6X6 mats when comparing furnish types within each of the three flake orientations. Among the mats with random flake orientation, the average shape factor of the YPMODEL mats was significantly less than that of both the YP6X6 and the COM6X6 mats. The average shape factor for the YP6X6 mats was also significantly less than that of the COM6X6 mats for the random flake orientation. For both directions of flake alignment, the average shape factor of the YPMODEL mats was significantly less than that of the COM6X6 mats. The relationship exhibited by the average void shape factor was similar to that of void diameter. The differences in shape factor between the different furnish types are the result of shorter, thicker voids being created when forming mats with commercial furnish. Shorter flake lengths create shorter void lengths, and thicker voids are created due to the increased amount of flake bridging that occurs when shorter flakes are deposited on top of one another. Figures 4a-c illustrate the proportion of mat area occupied by voids as a function of shape factor for the mats formed with flakes oriented randomly, parallel to the image plane, and perpendicular to the image plane, respectively. The differences in the distribution of void area when broken down by shape class are especially evident in the aligned orientations (Figs. 4b and c).

Tukey's HSD method ($\alpha = 0.05$) also uncovered significant differences in average shape factor between the three flake orientations for both the YPMODEL and COM6X6 mat types. For the YPMODEL mats, the average shape factors for both mats formed with randomly oriented flakes and mats formed with flakes oriented parallel to the image plane were significantly less than the average shape factor for

the mats formed with flakes oriented perpendicular to the image plane. The same trend was observed for the COM6X6 mats. The average shape factor for the mats formed with flakes parallel to the image plane was significantly less than that of both the randomly formed mats and the mats formed with flakes oriented perpendicular to the image plane. The randomly formed mats also had a significantly lower shape factor than those formed with flakes oriented perpendicular to the image plane. This indicates that preferential orientation of flakes caused significant differences in void shape. Flakes with their long axis oriented perpendicular to the image plane will generally have their shortest dimension parallel to the image plane, leading to the development of shorter, thicker voids during mat formation. These shorter thicker voids were responsible for the larger average shape factor exhibited by these mats. Inversely, flakes oriented parallel to the image plane generally have their longest dimension parallel to the image plane. This results in longer, thinner voids and a lower average shape factor. The randomly oriented mats exhibit an average shape factor that is intermediate to those of the aligned mats due to the mixture of void lengths and diameters created during mat formation.

Characterization charts for mat structure

Characterization charts are a common and effective means of summarizing the important parameters of a cellular material (Gibson and Ashby 1988). This format was used to create characterization charts for the mats evaluated in this experiment. A few of the terms were changed or omitted based on their relevance to the structure of wood flake mats, and to reflect the actual parameters that were measured with the quantification procedure outlined previously. Edge connectivity (Z) was taken to be the number of flakes meeting at the corner of a void in a mat. Table 3 presents characterization charts recorded for the mats in this study. The parameters listed were obtained from measurements made on images of

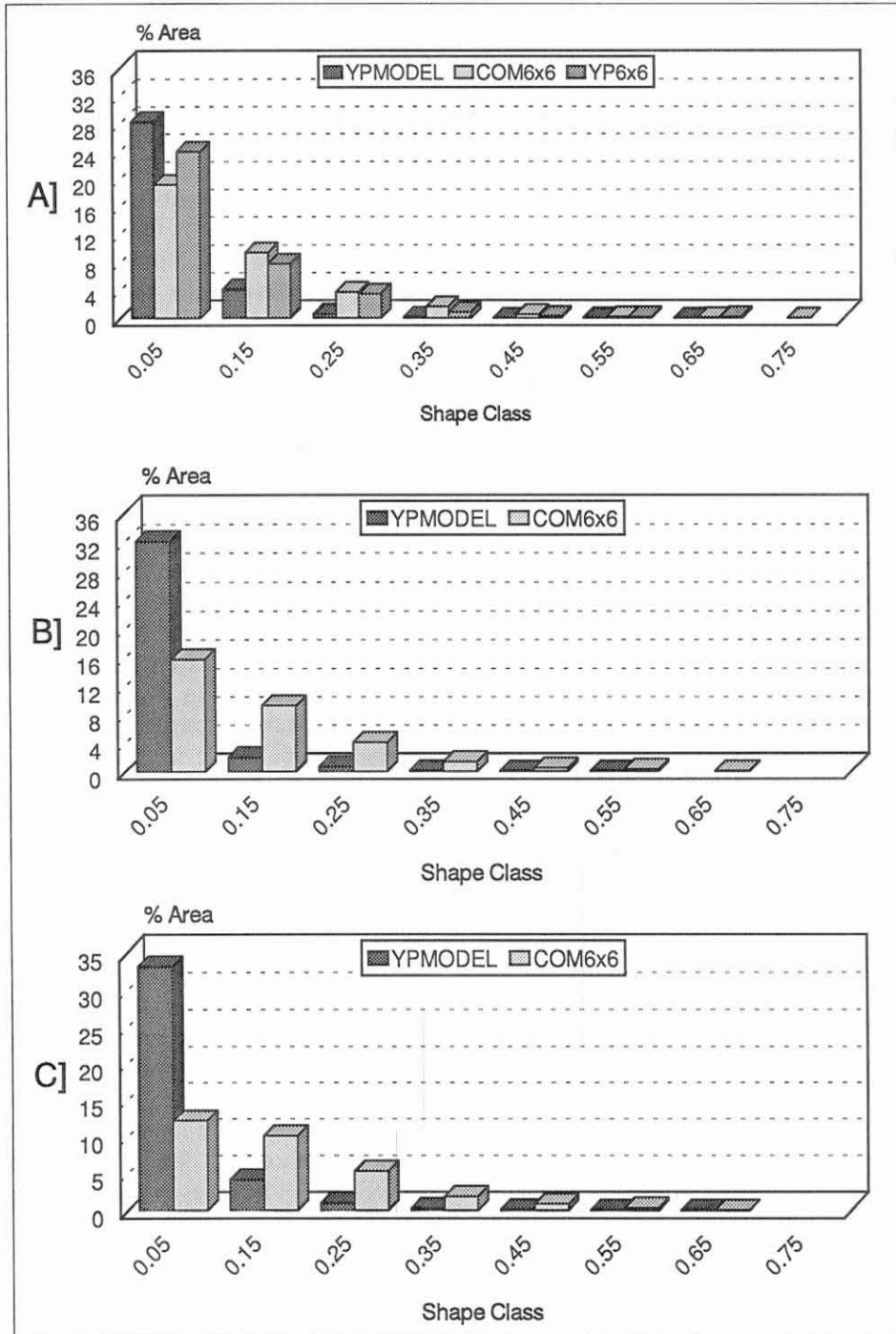


FIG. 4. Histograms depicting the distribution of void shape for: a) mats formed with flakes oriented randomly, b) mats formed with flakes oriented parallel to the image plane, and c) mats formed with flakes oriented perpendicular to the image plane.

TABLE 3. Characterization charts summarizing mat structural characteristics.

MAT TYPE Flake orientation	YPMODEL		
	Random	Parallel	Perpendicular
Raw material	Yellow-poplar	Yellow-poplar	Yellow-poplar
Density, ρ^* (kg/m ³)	250	250	250
Open or closed cells	Open	Open	Open
Edge connectivity, Z_e	2	2	2
Cell shape factor	0.12	0.10	0.15
Symmetry of structure	Anisotropic	Anisotropic	Anisotropic
Cell edge thickness, t_e (mm)	0.69	0.71	0.66
Longest chord, (mm)	12.47	14.83	10.96
Diameter, (mm)	0.51	0.45	0.54
Shape anisotropy ratio, $R_{LD} = /$	24.45	32.96	20.68
Standard deviation of void diameter (mm)	0.55	0.38	0.55
MAT TYPE	COM 6 × 6		
Flake orientation	Random	Parallel	Perpendicular
Raw material	Commercial	Commercial	Commercial
Density, ρ^* (kg/m ³)	250	250	250
Open or closed cells	Open	Open	Open
Edge connectivity, Z_e	2	2	2
Cell shape factor	0.27	0.25	0.29
Symmetry of structure	Anisotropic	Anisotropic	Anisotropic
Cell edge thickness, t_e (mm)	0.63	0.63	0.63
Longest chord, (mm)	6.43	6.61	5.23
Diameter, (mm)	0.71	0.68	0.73
Shape anisotropy ratio, $R_{LD} = /$	9.06	9.72	7.16
Standard deviation of void diameter (mm)	0.57	0.49	0.53
MAT TYPE	YP 6 × 6		
Flake orientation	Random		
Raw material	Yellow-poplar		
Density, ρ^* (kg/m ³)	250		
Open or closed cells	Open		
Edge connectivity, Z_e	2		
Cell shape factor	0.24		
Symmetry of structure	Anisotropic		
Cell edge thickness, t_e (mm)	0.70		
Longest chord, (mm)	8.07		
Diameter, (mm)	0.69		
Shape anisotropy ratio, $R_{LD} = /$	11.70		
Standard deviation of void diameter (mm)	0.58		

mat cross sections and from characterization of the furnish used.

CONCLUSIONS

A method for quantifying the cellular structure of a flakeboard mat has been presented and applied. The approach used considers the structure of a flakeboard mat to be that of a cellular material. Cross-sectional images of

narrow mat sections and small laboratory-size mats were obtained, and structural parameters were quantified using computer image analysis techniques. Mat structure was analyzed with respect to: the percent area of mat cross section occupied by voids, the size and shape of individual voids, and the distribution of void size and shape. Characterization charts were created to summarize the parameters critical to mat structure.

Computer image analysis provides an efficient and effective means of observing and quantifying the cellular structure of a wood flake mat from images of mat cross sections.

No significant differences in the percent areas of mat cross sections occupied by voids existed among the seven combinations of mat type and flake orientations studied.

The distributions of total void area separated into size classes are similar for all seven combinations of mat type and flake orientation. These distributions are fairly uniform in shape, with the largest proportions of void area being occupied by voids in the 0 to 10 mm² and > 100 mm² size classes in all cases. Most voids that are greater than 100 mm² in area are aggregate voids resulting from connections between adjacent voids.

For mats formed with the long axis of the flakes oriented perpendicular to the plane of the image, YPMODEL mats have significantly larger average void area than COM6X6 mats. No significant differences in average void area exist between the three mat types for mats formed with flakes oriented randomly and parallel to the plane of the image. Within each of the three mat types, no significant differences in average void area exist between the three different directions of flake orientation.

The influence of shorter flakes during the formation of mats from commercial furnish has a significant effect on the shape of the voids created. Voids in COM6X6 mats have significantly larger diameters and shorter chord lengths than voids in YPMODEL mats within each of the three flake orientations. This difference is manifested in the void shape factor, which is significantly less for the YPMODEL mats than for the COM6X6 mats at each of the three flake orientations. Randomly oriented YP6X6 mats exhibit an average shape factor that is significantly greater than that of YPMODEL mats and significantly less than that of COM6X6 mats.

Flake orientation also has a significant effect on void shape. For the YPMODEL mats, those with the flakes oriented perpendicular to the image plane have a significantly larger average

shape factor than mats with the flakes oriented both randomly and parallel to the image plane. For the COM6X6 mats, the average shape factor of mats formed with flakes oriented parallel to the image plane is significantly less than that for randomly oriented mats, which in turn is significantly less than the average shape factor for mats formed with flakes oriented perpendicular to the image plane.

The experimental findings indicate that although significant differences in some mat structural parameters exist between the model mats and the more realistic square mats, both mat types will be useful in subsequent investigations of the stress-strain behavior of wood flake mats during consolidation. During consolidation of a wood flake mat, the stress-strain behavior involves the compression of continuous flake columns and the bending of flakes that span voids. Differences in void sizes and shapes certainly impact these mechanisms. The results of this study provide a basis for establishing a conceptual model of the compressive stress-strain behavior of wood flake mats.

ACKNOWLEDGMENTS

The authors wish to acknowledge Professor Michael P. Wolcott at West Virginia University for his important participation in this work and Weyerhaeuser, Elkin, NC, for supplying commercial OSB furnish. Funding was provided by the USDA Competitive Grants program, project #91-37103-6642.

REFERENCES

- ASHBY, M. F. 1983. The mechanical properties of cellular solids. *Metal. Trans. A.* 14A:1755-1769.
- DAI, C., AND P. R. STEINER. 1994a. Spatial structure of wood composites in relation to processing and performance characteristics. Part II. Modelling and simulation of a randomly-formed flake layer network. *Wood Sci. Technol.* 28:135-146.
- , AND ———. 1994b. Spatial structure of wood composites in relation to processing and performance characteristics. Part III. Modelling and simulation of a multi-layered random strand mat. *Wood Sci. Technol.* 28:229-239.
- GIBSON, L. J. 1989. Modeling the mechanical behavior of cellular materials. *Mat. Sci. Eng.* A110(1989):1-36.

- , AND M. F. ASHBY. 1988. Cellular solids: Structure and properties. Pergamon Press, New York, NY.
- HARLESS, T. E. G., F. G. WAGNER, P. H. SHORT, R. D. SEALE, P. H. MITCHELL, AND D. S. LADD. 1987. A model to predict the density profile of particleboard. *Wood Fiber Sci.* 19(1):81–92.
- KELLY, M. 1977. Critical review of the relationships between processing parameters and physical properties of particleboard. USDA Forest Prod. Lab. Gen. Tech Rep. FPL 10:1–65. Madison, WI.
- LANG, E. M., AND M. P. WOLCOTT. 1996. A model for the viscoelastic consolidation of wood-strand mats. Part I. Structural characterization of the mat via Monte Carlo simulation. *Wood Fiber Sci.* 28(1):100–109.
- MEINEKE, E. A., AND R. C. CLARK. 1973. Mechanical properties of polymeric foams. Technomic, Westport, CT.
- STEINER, P. R., AND C. DAI. 1994. Spatial structure of wood composites in relation to processing and performance characteristics. Part I. Rationale for model development. *Wood Sci. Technol.* 28:45–51.
- SUCHSLAND, O. 1959. An analysis of the particleboard process. *Quart. Bull. Michigan Agric. Exp. Sta. Michigan State Univ.* 42(2):350–372.
- . 1962. The density distribution in flakeboard. *Quart. Bull. Michigan Agric. Exp. Sta., Michigan State Univ.* 45(1):104–121.
- , AND H. XU. 1989. A simulation of the horizontal density distribution in a flakeboard. *Forest Prod. J.* 39(5): 29–33.
- , AND ———. 1991. Model investigations of the particle bonding process. Michigan State University Dept. of Forestry, East Lansing, MI.
- UNIVERSAL IMAGING. 1991. Image-1 function guide. Universal Imaging Corp., Westchester, MA.
- WARREN, W. E., AND A. M. KRAYNIK. 1987. Foam mechanics: The linear elastic response of two-dimensional spatially periodic cellular materials. *Mech. Mat.* 6:27–37.
- WOLCOTT, M. P. 1989. Modeling viscoelastic cellular materials for the pressing of wood composites. Ph.D. dissertation, Virginia Polytechnic Inst. and State Univ., Blacksburg, VA.
- , F. A. KAMKE, AND D. A. DILLARD. 1990. Fundamentals of flakeboard manufacture: Viscoelastic behavior of the wood component. *Wood Fiber Sci.* 22(4): 345–361.